ELSEVIER

Available online at www.sciencedirect.com
SCIENCE DIRECT

Ultramicroscopy 100 (2004) 339–346

ultramicroscopy

www.elsevier.com/locate/ultramic

Characterization of self-assembling isolated ferroelectric domains by scanning force microscopy

Bongki Lee[a], Changdeuck Bae[a], Seung-Hyun Kim[b], Hyunjung Shin[a,*]

[a] *School of Advanced Materials Engineering, Kookmin University,861-1,Chengnun-dong, Seoul, 136-702, Republic of Korea*
[b] *Inostek Inc., Seoul, 153-023, Republic of Korea*

Received 1 July 2003; received in revised form 1 December 2003; accepted 2 December 2003

Abstract

Lead zirconate titanate (PZT) thin films were prepared by a sol–gel process on platinized Si substrate. Their microstructure and surface morphology were characterized by XRD and Scanninn Force Microscopy. Phase transformation of the prepared PZT films from pyrochlore to ferroelectric was observed by XRD and PFM (piezoresponse force microscopy), respectively. Self-assembling nano-structured ferroelectric phases are fabricated by solution deposition technique followed by the controlling kinetics of the transformation. Complex structures of ferroelectric domains in the isolated ferroelectric phases were found in the furnace annealed PZT films in the temperature range of 400–500°C. Single ferroelectric domain structure in the isolated ferroelectric phases could be found in thinner PZT films and used to study the size effect of laterally confined ferroelectric domains.
© 2004 Elsevier B.V. All rights reserved.

1. Introduction

Ferroelectric thin film materials show broad range of their unique properties, such as high dielectric permittivity, high piezoelectric constants and electromechanical coupling, and high pyroelectric coefficients, etc. and enjoy being many useful components [1,2]. More recently, these materials have been intensively studied due to their promising applications in microelectronic devices as well as in smart-sensing and self-actuating-micro-systems. Advanced devices and systems are getting smaller and smarter, nano-structured multi-functional materials, for example isolated dots and ultra thin films of lead zirconate titanate (PZT, $Pb(Zr_xTi_{1-x})O_3$) as well as many other ferroelectrics, need to be prepared and characterized.

Immediate fundamental issue, therefore, is the scaling limitation of ferroelectric switching in nanometer scale (<100 nm) [3]. Over 25 years the theoretical works have been done to estimate the minimum ferroelectric film thickness and few experimental works, realized only in recent, below in 100 nm in thickness, which is impetus for the current investigation [4,5]. The investigations of size effects in ferroelectric films were focused on the dependencies of films' thickness, not on the lateral dimension [6,7]. Notable example is the drastic increase of coercive field below a critical thickness, as has been found in some polycrystalline thin films [8]. However, it has been found that

*Corresponding author. Tel.: +82-31-910-4897; fax: +82-31-910-4320.
E-mail address: hjshin@mail.kookmin.ac.kr (H. Shin).

0304-3991/$ - see front matter © 2004 Elsevier B.V. All rights reserved.
doi:10.1016/j.ultramic.2003.12.015

even under the same processing conditions, change in film thickness can lead to a change in grain size [9]. The stability of individual domains as a function of film thickness and microstructure, mainly grain size, were also investigated. In recent publications [10,11], they have been shown by Transmission electron microscopy (TEM) investigations that grain size, not the thickness, is the primary factor governing the domain structure and consequently the electrical properties. Therefore, fabrication and control of the single domain in a laterally confined nanostructure is of importance to elucidate the size effect in ferroelectrics. Ramesh's research group in University. of Maryland, USA, investigated the ferroelectric and piezoelectric properties of sub-micron sized ferroelectric devices. E-beam lithography and focused ion-beam milling were utilized to fabricate the nano-devices as small as 90×90 nm of Pt/$SrBi_2Ta_2O_9$/Pt and Pt/LSCO[$(La_{0.5}\ Sr_{0.5})CoO_3$]/PNZT[$Pb_{1.0}(Nb_{0.04}Zr_{0.28}Ti_{0.68})O_3$]/LSCO/Pt [12,13]. With shrinking dimensions, the side-wall damage by the reactive etching processes will become more important and should be addressed in an adequate manner. More interestingly, Alexe's group in Germany fabricated self-assembled nano-electrodes of δ-Bi_2O_3 on $Bi_4Ti_3O_{12}$/$SrTiO_3$ [14–16]. The self-assembled nano-cell was in the size of 0.18 μm in diameter. In both groups, scanning force microscopy (SFM) makes possible to analyze their ferroelectric and piezoelectric properties of the nano ferroelectric capacitor cells.

Several research groups have been also explored the chemical solution deposition technique, that a precursor solution containing metal-organic molecules in either aqueous or organic solvent is used to form a solid precursor film on a substrate by either spin coating or dip-coating. The precursor film is pyrolyzed followed by crystallized with a heat treatment to form a polycrystalline thin film. Many studies of PT ($PbTiO_3$), PZT, and PLZT ($(Pb,La)(Zr,Ti)O_3$) films report a metastable intermediate, known as "pyrochlore", phase at lower temperatures [17]. It is a well-known fact that the kinetically stable "pyrochlore" phase degrades overall ferroelectric properties of the films [18]. Therefore, most investigations are mainly focused on the elimination of the "pyrochlore" phase. In this work, however, the metastable phase will be utilized as non-ferroelectric matrix containing isolated ferroelectric islands. Chemical solution deposition provides a great chance to grow or fabricate isolated and self-assembled ferroelectric islands by controlling the growth kinetics.

Recently, SFM has emerged as a powerful tool for analysis of nanometer-sized objects in surfaces and further improvement provides many other SFMs, based on magnetic, electric, mechanical, and piezoelectric interaction between the tip and the surfaces. In comparison with other analytical characterization techniques, such as TEM as well as Scanning Electron Microscopy (SEM), SFM can provide more information by allowing the study of 3D geometry and better statistics with larger area scanning. Above all sample preparation for SFM is much easier and all kinds of flat surfaces can be characterized.

Spatial inhomogeneity in ferroelectric films at the nanometer scale became recently an important issue due to the increasing efforts to scale down to be integrated them with the advanced memory devices as well as sensors and actuators in smart microsystems [19]. Until now, functionality of the ferroelectric materials has been interpreted using microstructural characterization techniques combined with their properties' measurements in macroscopically. As feature size decreases, however, local probe techniques become essential.

SFM has opened up a new vista of research into the nanoscopic responses of ferroelectric materials [20–22]. Particularly, SFM in the piezoresponse detection mode has been employed recently as an effective tool for visualization of domain structure in ferroelectric thin films together with their surface morphology [23–24]. This technique allows non-destructive and high-resolution domain imaging as well as local piezoelectric measurements [25–28]. Several groups [29,30] have demonstrated the ability to explore and exploit the inverse piezoelectric effect that is available through the interaction ferroelectric materials and the AC signal imposed on the SFM tip. In very recent, using local piezoelectric measurement technique, Roelof et. al. [31] differentiated 180° and 90° domains switching in ferroelectric polycrystalline

PT films. Fatigue studies using this technique are notable examples [32]. Colla et. al. [33] recently observed ''ferroelectrically dead'' regions in fatigued PZT films. The ability to probe the microscopic details and to write a sub-100 nm ''artificial domain'' has already been demonstrated in continuous thin films and heterostructures, in which the in-plane dimensions are much larger (essentially infinite) compared to the thickness dimension [34–36]. In this work, isolated ferroelectric dots are investigated by the SFM in the piezoresponse detection mode.

Fabrication and investigation of the domain in a laterally confined nanostructure is of importance to elucidate the size effect in ferroelectric materials. In this study, the isolated nanostructures were prepared in the course of microstructural development in the sol–gel processed PZT ($Pb(Zr_{0.52}Ti_{0.48})O_3$) thin films and characterized them by the piezoresponse mode of SFM — hereafter piezoresponse force microscopy (PFM).

2. Experimental procedure

Platinized silicon ($Pt/Ti/SiO_2/Si$) substrates were used to prepare the PZT films and the evolution of ferroelectric phase. Ferroelectric thin films were deposited using a sol–gel process. Sol solutions were prepared with Zr/Ti = 52/48 and Pb content was 10% in excess of stoichiometry. The solutions were then spun onto the platinized Si substrates at 4000 rpm for 30 s. The spun film samples were pyrolyzed on a hot plate below 300°C for 5 min. followed by each layer of deposition. In this study, the films of about 300 nm in thickness were prepared by 6 consecutive depositions.

The prepared PZT thin films were annealed by two different ways. One was annealing in the conventional tube furnace (hereafter FA) with heating rate of 20°C/min up to 400–650°C, and held for 5 min–60 min. The other used a home-built rapid thermal annealing equipment (hereafter RTP) up to 400–650°C, and held for 5 min–60 min.

Crystallinity and microstructural characterization was performed using X-ray diffractometer (Bruker, D8 Discovery with GADDS) and small angle diffraction was utilized to investigate the near surfaces of the films.

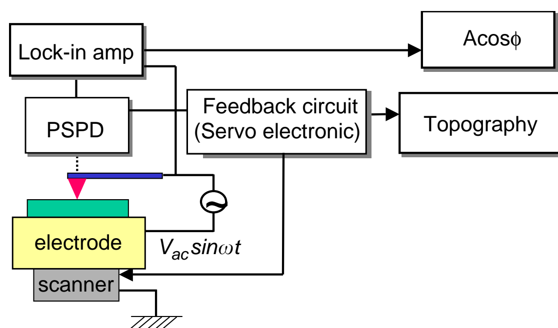

Fig. 1. Schematic diagram for the experimental set of PFM

Scanning force microscopy (Seiko SPA 400, Japan) was used to characterize the surface morphology of the films as well as the piezoelectric response from the self-assembling isolated ferroelectric domains in nanometer scale. Conductive SFM tips used are made of either boron doped p-type Si or metal-coated (Pt or/and Au) Si tips. The radius of tip curvature was reported to be 10 nm by vendor (NT-MDT, Russia).

Experimental set up for PFM to characterize the ferroelectric films at the nanometer scale is shown in the Fig. 1. Briefly, a conductive tip probes the sample surface with an arbitrary frequency in the kHz range (in this work 10 kHz was used) as a reference signal is applied between the tip and the bottom electrode of the ferroelectric films. Due to the converse piezoelectric effect, the sample underneath the tip mechanically oscillates with the same frequency as the excitation signal and thus generates oscillations of the cantilever. Using a frequency modulation with a lock-in amplifier, the piezoelectric signal is extracted from the total deflection signal of the cantilever. All piezoelectric measurements were performed in a contact mode of SFM at room temperature and ambient pressure.

3. Results and discussion

XRD experimental results are summarized in Table 1. For the PZT films of RTP annealed at different annealing temperatures holding for

Table 1
XRD results of RTP and FA PZT films

	Nucleation temperature of Perovskite (°C)	Fully Perovskite (°C)	Preffered orientation of Perovskite
RTP	550	600	(1 1 0),(1 0 1)
FA	500	550	(1 1 0),(1 0 1) (1 0 0)

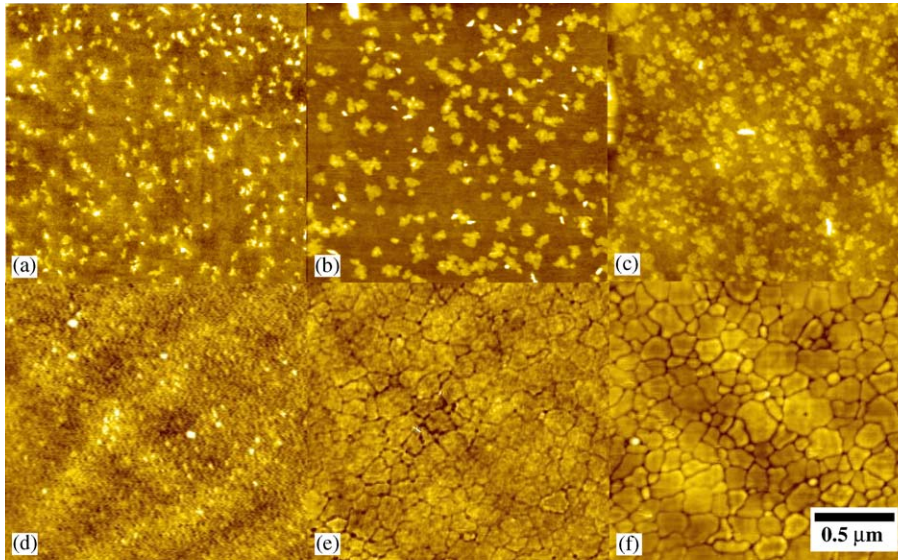

Fig. 2. (a)–(f) Scanning force micrographs of RTP PZT films' surfaces annealed at (a) 400°C, (b) 450°C, (c) 500°C, (d) 550°C, (e) 600°C and (f) 650°C for 30 min. respectively.

30 min, pyrochlore phases are found in the samples at 500°C and 550°C. Between 550°C and 600°C, phase mixture of pyrochlore and ferreoelectric has been observed. Above 600°C only ferroelectric phases with (1 1 0) or (1 0 1) preferred orientations are found.

For the FA PZT films at different annealing temperatures for 30 min, in contrary, pyrochlore phases are found at 500°C. Between 500°C and 550°C, the phase transition from pyrochlore to ferreoelectric has occurred. It is noted that the transition temperature in furnace annealing was lower than RTP annealing one. Above 550°C, ferroelectric phases with both (1 0 0) and (1 1 0) or (1 0 1) preferred orientations are found in the XRD experiments. According to small angle (incident angle of 5°) XRD experimental results, more (1 0 0)-oriented ferroelectric phases are observed and small portion of pyrochlore phases is found in the near surface of the FA PZT films. It implies that the (10 0)-oriented PZT started to be nucleated at the Pt surface and grew to the outer surface. Even at high-temperature annealing (higher than 650°C) in the surface of the FA films, kinetically more stable pyrochlore phases are found to be remaining as a shoulder of PZT (1 1 0), (1 0 1) peaks found in the small angle XRD results.

Fig. 2 show the series of surface morphologies in RTP annealed PZT films in the range from 400°C to 650°C, respectively. RTP annealed PZT films at 400°C, 450°C, and 500°C show transformed pyrochlore phases as white "floral" particles in the amorphous phase, which is agreed well with

the results from XRD. The transformed ferroelectric phase at 500°C was, however, barely detected by XRD. At 550°C, the phase transformation from pyrochlore phase to ferroelectric phase is undergone. Smooth surfaces shown in Fig. 2(d) indicated the ferroelectric phases are started to nucleate underneath of pyrochlore phases. It is proposed that the surface is covered with pyrochlore phases and the ferroelectric phases are nucleated near the interface between the substrate and the film. This observation was also confirmed by small angle XRD as mentioned above. At higher temperature than 600°C, the pyrochlore phases never appeared in the rapid thermal annealing, whereas only well-developed and distinct equiaxed ferroelectric grains were found.

In the case of FA films, which the heating rate (20°C/min) is slower than RTP, the formation of kinetically more favorable pyrochlore phases is unavoidable. Fig. 3 present the series of surface morphologies in FA annealed PZT films from 400°C to 650°C, respectively. Featureless surface topography was found in FA PZT at 400°C shown in Fig. 3(a). In Fig. 3(b) transformed ferroelectric phases were observed as white particles, which are barely detected by XRD. Diameter and height of the ferroelectric phases were about 50 and 20 nm, respectively. At higher than 550°C, the so-called, "rosette" structured grains were observed in SFM topographies shown in Figs. 3(d)–(f). Rougher surface morphology (6.7 nm in roots mean square(rms)) and larger grains than the equi-axed grained RTP PZT surfaces (1.2 nm in rms) characterized the Rosette structure in Fig. 3(f).

Fig. 4(a)–(f) show surface topographies and PFM images from FA PZT films at 430°C, 450°C and 470°C, respectively, for 60 min. As a result, between at the temperature of 400°C and 500°C, the self-assembled ferroelectric phases are formed in the pyrochlore phase. As the annealing temperature increased, the sizes of ferroelectric phases in pyrochlore are also increased from about 200 to 460 nm in diameter and the coverage of the transformed ferroelectric phases is also increased. Impingement of each ferroelectric grain can be observed at higher temperature than 450°C. The isolated ferroelectric domains exhibit piezoresponse, which dark and bright contrasts indicate two opposite ferroelectric domains interacting with the applied AC modulation voltage, whereas the surroundings of pyrochlore phase show non-piezoresponse activities as shown in Figs. 4(b), (d) and (f). At 470°C, each ferroelectric phase contain

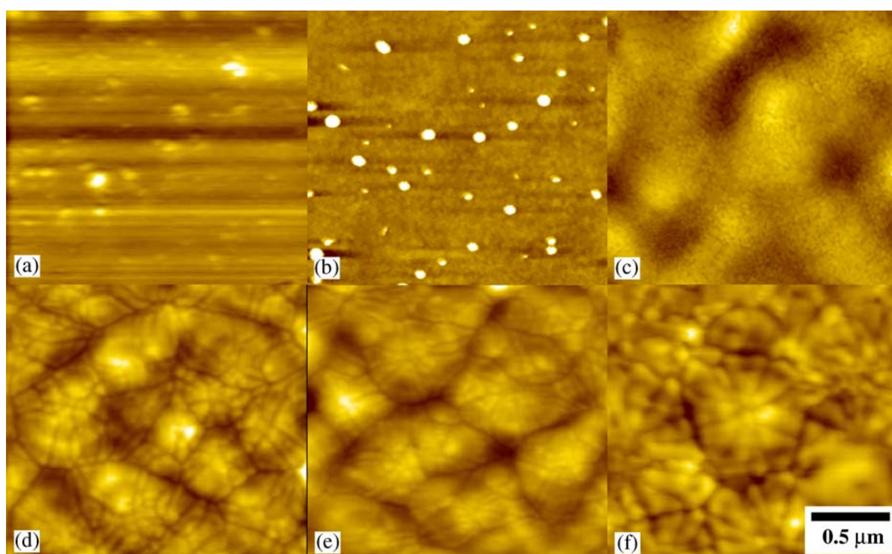

Fig. 3. (a)–(f) Scanning force micrographs of FA PZT films' surfaces annealed at (a) 400°C, (b) 450°C, (c) 500°C, (d) 550°C, (e) 600°C and (f) 650°C for 30 min, respectively.

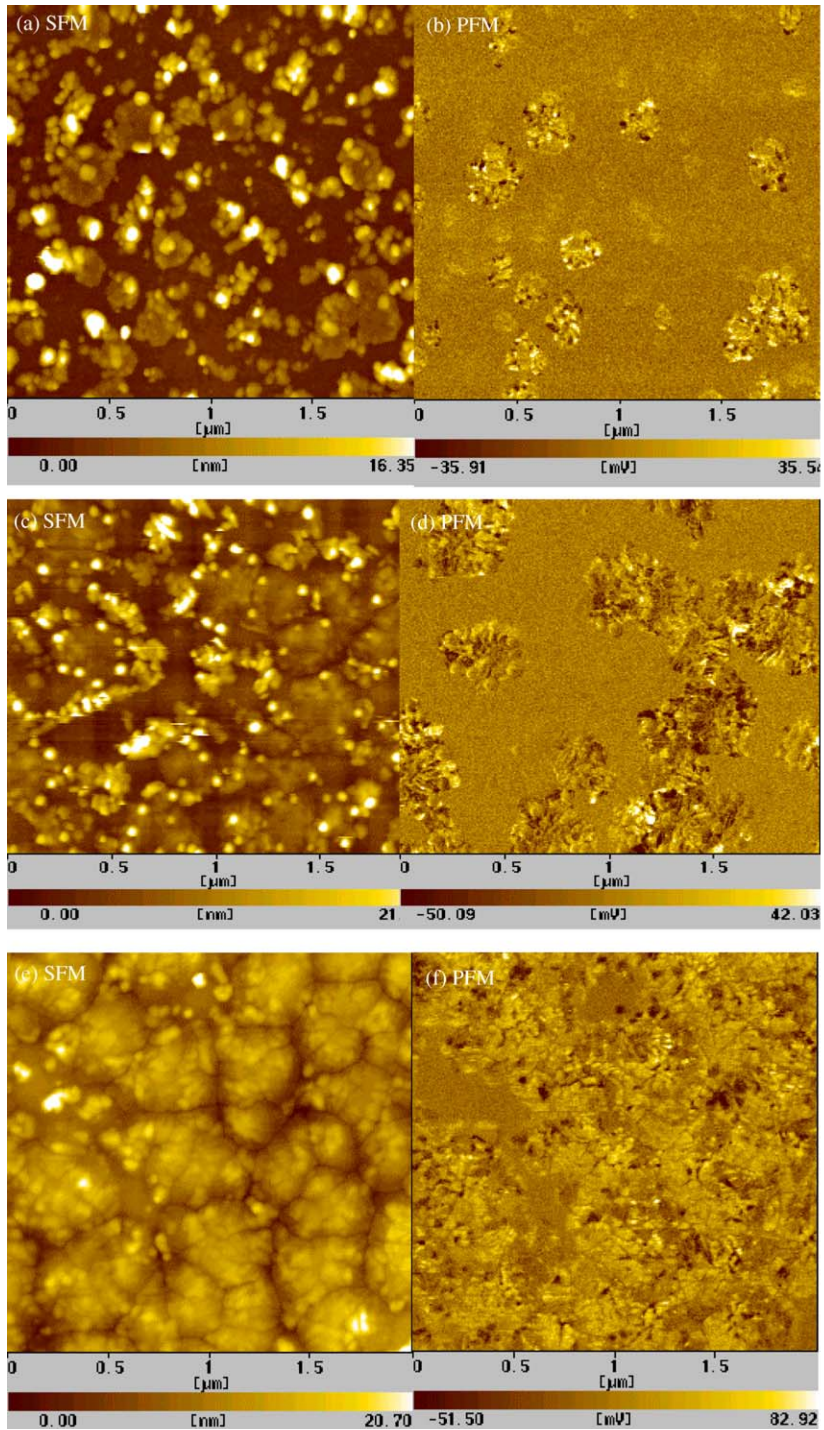

Fig. 4. (a)–(f) SFM topographies and PFM images of FA PZT films at 430°C, 450°C and 470°C for 60 min. respectively.

several ferroelectric domains with complex orientations shown in Fig. 4(f). It is noted that the single grain containing the single ferroelectric domain was hardly found. It is implied that the multi-domain structures are more stable than the single-domain structure in the isolated ferroelectric grains, which are larger than 100 nm in diameter. Smaller grain is still covered by pyrochlore phases, thereby weak piezoresponse signal prevent observing the single domain in the single grain as shown in Fig. 4(b). It is suggested that thinner PZT films (<100 nm) required to form a structure of stable single ferroelectric domain.

4. Conclusions

PZT thin films were prepared by chemical solution deposition and their microstructural developments were characterized by XRD and SFM. Two different annealing methods were investigated to fabricated isolated ferroelectric phases in the surroundings of non-ferroelectric phases, i.e. pyrochlore phases. The isolated ferroelectric phases in the diameter of about 200–500 nm were found in FA PZT films at 430°C, 450°C and 470°C. Local probing technique such as SFM in the piezoresponse mode is utilized to analyze their piezoelectric properties and to image their ferroelectric domain structures with very high resolution. Piezoresponse mode of SFM shows complex ferroelectric domains in the isolated phase, not from the surroundings. Single ferroelectric domain in the single grain could be obtained in the PZT films thinner than 100 nm in thickness.

Acknowledgements

The financial support of Kookmin University and National R&D Project for Nano Science and Technology through Seoul National University is gratefully acknowledged. S.-H. Kim also thanks to National Research Laboratory(Electronic Materials Lab.) for their financial support in part. The authors would also like to thank Prof. J. Kim and J.G. Lee from Kookmin University for their encouragements and stimulus discussion.

References

[1] J.F. Scott, Ferroelectrics Rev. 1 (1) (1998) 1.
[2] N. Setter, R. Waser, Acta Mater. 48 (2000) 151.
[3] T.M. Shaw, S. Troiler-McKinstry, P.C. McIntyre, Annu. Rev. Mater. Sci. 30 (2000) 263.
[4] A.V. Bune, et al., Nature 391 (1998) 874.
[5] C.H. Lin, P.A. Friddle, X. Lu, H. Chen, Y. Kim, T.B. Wu, Appl. Phys. Lett. 88 (4) (2000) 2157.
[6] Y. Sakashita, H. Segawa, K. Tominaga, M. Okada, J. Appl. Phys. 73 (11) (1993) 7857.
[7] K.R. Udayakumar, P.J. Schuele, J. Chen, S.B. Krupanidhi, L.E. Cross, J. Appl. Phys. 77 (8) (1995) 3981.
[8] J.F. Scott, C.A. Araujo, L.D. McMillan, Ferroelectrics 140 (1993) 219.
[9] Y. Sakashita, H. Segawa, K. tominaga, M. Okada, J. Appl. Phys. 73 (11) (1993) 7857.
[10] S.B. Ren, C.J. Lu, J.S. Liu, H.M. Shen, Y.N. Wang, Phys. Rev. B 54 (20) (1996) R14337.
[11] S.B. Ren, C.J. Lu, H.M. Shen, Y.N. Wang, Phys. Rev. B 55 (6) (1997) 3485.
[12] C.S. Ganpule, A. Stanishevsky, S. Aggarwal, J. Melngailis, E. Williams, R. Ramesh, Appl. Phys. Lett. 75 (24) (1999) 3874.
[13] C.S. Ganpule, A. Stanishevsky, Q. Su, S. Aggarwal, J. Melngailis, E. Williams, R. Ramesh, Appl. Phys. Lett. 75 (3) (1999) 409.
[14] M. Alexe, J.F. Scott, C. Curran, N.D. Zakharov, D. Hesse, A. Pignolet, Appl. Phys. Lett 73 (11) (1998) 1592.
[15] M. Alexe, A. Gruvermann, C. Haenagea, N.D. Zakharov, A. pignolet, D. Hesse, J.F. Scott, Appl. Phys. Lett. 75 (8) (1999) 1158.
[16] M. Alexe, C. Haenagea, D. Hesse, U. Gösele, Appl. Phys. Lett 75 (12) (1999) 1793.
[17] A. Seifert, F.F. Lange, J.S. Speck, J. Mater. Res. 10 (3) (1995) 680.
[18] T. Tani, D.A. Payne, J. Am. Ceram. Soc. 77 (5) (1994) 1242.
[19] A. Gruvermann, Appl. Phys. Lett. 75 (10) (1999) 1452.
[20] F. Saurenbach, B.D. Terris, Appl. Phys. Lett. 56 (1990) 1703.
[21] O. Kosolov, A. Gruvermann, J. Hatano, K. Takahashi, H. Tokumoto, Phys. Rev. Lett. 74 (1995) 4309.
[22] G. Zavala, J.H. Fendler, S. Troiler-McKinstry, J. Appl. Phys. 81 (1997) 7480.
[23] O. Auciello, A. Gruverman, H. Tokumoto, S.A. Prakash, S. Aggarwal, R. Ramesh, MRS Bull. 23 (1) (1998) 33.
[24] A. Gruverman, H. Tokumoto, A.S. Prakash, S. Aggarwal, B. Yang, R. Ramesh, O. Auciello, T. Venkatesan, Appl. Phys. Lett. 71 (1997) 3492.

[25] P. Guethner, K. Dransfield, Appl. Phys. Lett. 61 (1992) 1137.
[26] T. Hidaka, T. Maruyama, M. Saitoh, N. Mikoshiba, M. Shimizu, T. Shiosaki, L.A. Wills, R. Hiskes, S.A. Dicarolis, J. Amano, Appl. Phys. Lett. 68 (1996) 2358.
[27] J.A. Christman, R.R. Woolcott Jr, A.I. Kingon, R.J. Nemanich, Appl. Phys. Lett. 73 (26) (1998) 3851.
[28] G.D. Hu, J.B. Xu, I.H. Wilson, Appl. Phys. Lett. 75 (1) (1999) 1610.
[29] L.M. Eng, Nanotechnology 10 (1999) 405.
[30] C. Durkan, M.E. Well, D.P. Chu, P. Migliorato, Phys. Rev. B 60 (23) (1999) 16198.
[31] A. Roelofs, U. Bottger, R. Waser, F. Schlaphof, S. Trogisch, L.M. Eng, Appl. Phys. Lett. 77 (21) (2000) 3444.
[32] A. Gruverman, O. Auciello, H. Tokumoto, Appl. Phys. Lett. 69 (1996) 3191.
[33] E.L. Colla, S. Hong, D.V. Taylor, A.K. Tangantsev, N. Setter, Appl. Phys. Lett. 72 (1997) 2478.
[34] C.H. Ahn, T. Tybell, L. Antognazza, K. Char, R.H. Hammond, M.R. Beasley, O. Fischer, J.-M. Triscone, Science 276 (1997) 1100.
[35] A. Gruverman, O. Auciello, H. Tokumoto, J. Vac. Sci. Technol. B 14 (2) (1996) 602.
[36] T. Maruyama, M. Saitoh, I. Sakai, T. Hidaka, Y. Yano, T. Noguchi, Appl. Phys. Lett. 73 (1998) 3524.